TYPE Original Research
PUBLISHED 29 October 2025
DOI 10.3389/fbuil.2025.1701378



#### **OPEN ACCESS**

EDITED BY Binbin Yang, Xuchang University, China

REVIEWED BY
Shengwen Tang,
Wuhan University, China
Faisal Al-Maqate,
Umm al-Qura University, Saudi Arabia

\*CORRESPONDENCE Radek Ševčík, ⋈ sevcik@itam.cas.cz

RECEIVED 08 September 2025 ACCEPTED 13 October 2025 PUBLISHED 29 October 2025

#### CITATION

Ševčík R, Kolář M, Pokorný J, Zárybnická L, Honzíček J and Machotová J (2025) Polymeric bio-based nanodispersed admixtures for the production of hydrophobic Portland cement mortars. Front. Built Environ. 11:1701378. doi: 10.3389/fbuil.2025.1701378

#### COPYRIGHT

© 2025 Ševčík, Kolář, Pokorný, Zárybnická, Honzíček and Machotová. This is an open-access article distributed under the terms of the Creative Commons Attribution License (CC BY). The use, distribution or reproduction in other forums is permitted, provided the original author(s) and the copyright owner(s) are credited and that the original publication in this journal is cited, in accordance with accepted academic practice. No use, distribution or reproduction is permitted which does not comply with these terms.

# Polymeric bio-based nanodispersed admixtures for the production of hydrophobic Portland cement mortars

Radek Ševčík<sup>1,2</sup>\*, Martin Kolář<sup>3</sup>, Jaroslav Pokorný<sup>2</sup>, Lucie Zárybnická<sup>1</sup>, Jan Honzíček<sup>3</sup> and Jana Machotová<sup>3</sup>

<sup>1</sup>Institute of Theoretical and Applied Mechanics of the Czech Academy of Sciences, Prague, Czechia, <sup>2</sup>Department of Civil Engineering, Faculty of Technology, Institute of Technology and Business, České Budějovice, Czechia, <sup>3</sup>Faculty of Chemical Technology, Institute of Chemistry and Technology of Macromolecular Materials, University of Pardubice, Pardubice, Czechia

A current trend in the construction industry involves the development and employment of eco-friendly, durable, and sustainable materials. Numerous admixtures, including various polymers, are used to modify the properties of cement. Nonetheless, their effectiveness and environmental impacts are still a matter of discussion. In this context, this work was focused on the application of innovative vegetable oil-based polymeric nanodispersed admixtures, synthesized following green chemistry principles, such as using water as a solvent. The synthesized bio-based latex admixtures were incorporated with 30 wt% of vegetable oil-based monomers derived from camelina, linseed, and rapeseed oils. The produced ordinary Portland cement fine-grained mortars, containing 0.1 wt% of each bio-based latex admixture, were thoroughly examined using several instrumental methods, such as isothermal calorimetry and scanning electron microscopy, to gain a comprehensive understanding of the roles of bio-based latex admixtures on the physical, mechanical, and microstructural properties of the examined specimens. It was found that the addition of bio-based latex admixtures led to changes in the hydration process, mineralogical composition, and liquid water transport. For example, the water absorption coefficient was found to be approximately 40% lower compared to cement mortars produced using a reference latex additive without the vegetable oil-based component. Moreover, cement mortars with a bio-based latex admixture containing camelina oil exhibited comparable compressive strength to those produced solely from ordinary Portland cement. Thus, the newly developed bio-based polymeric nanodispersion represents a new class of environmentally friendly admixtures that may be effectively utilized for water-loaded structures.

KEYWORDS

 $bio-based\ polymer, latex\ admixture,\ nanodispersions,\ portland\ cement,\ microstructure,\ water\ transport$ 

## 1 Introduction

Cement-based materials are commonly used in construction due to their economic viability, durability, and versatility, which enable the shaping of diverse objects

through casting (Barbhuiya et al., 2025). This quality differentiates them from other construction materials (Li G. et al., 2021). However, ordinary cementitious objects are heterogeneous and brittle materials with flaws, such as poor toughness, flexibility, and volume change (Van Tittelboom and De Belie, 2013; Fan et al., 2023). Various methods were proposed to address the drawbacks mentioned above and extend the overall service life of cementbased structures, such as the use of polymer admixtures (Ramli and Akhavan Tabassi, 2012). Polymer modification of cement-based materials was usually done by adding a film-forming polymer latex as a re-dispersible powder or by blending cement with an aqueous polymer dispersion. Modification was achieved through a combination of cement hydration and the formation of a polymer film (Liu Q. et al., 2023). Finally, a composite matrix consists of inorganic phases formed during cement hydration and an organic phase, such as a polymer film (Wagner, 1965; Ohama, 1998).

Polymer latexes comprise a large group of materials that are widely used to positively influence various properties of cementitious materials, including workability, adhesion, crack resistance, durability, and water transport (Jenni et al., 2006; Kong et al., 2013; Ali et al., 2021; Bilal et al., 2021). Various synthetic polymer latexes were used as cement modifiers. Styrenebutadiene (SBR) latex was found to have a positive effect on the workability of fresh-state mortar and the flexural strength of the hardened composites (Barluenga and Hernández-Olivares, 2004; Ukrainczyk and Rogina, 2013; Baueregger et al., 2015; Sun et al., 2019). Portland cement mortars modified with SBR latex exhibited improved long-term impermeability to water and carbon dioxide (Eren et al., 2017). Polyacrylic ester (PAE) latex provided better abrasion resistance and durability of cement mortars (Jiang et al., 2018). Styrene-acrylic ester copolymer (SAE) latex (Wang and Wang, 2010) enhanced the mortar's toughness, shrinkage resistance, and water impermeability. SAE and SBR were also found to reduce the fluidity loss rate and prolong the setting time of cement pastes (Shi et al., 2021). Ethylene-vinyl acetate (EVA) latexes were also widely used for the modification of concrete and mortar. Their application influenced the hydration kinetics of Portland cement (Silva et al., 2002; Betioli et al., 2012). Epoxy latexes were used to improve the flexural strength of hardened Portland cement concrete (Li P. et al., 2021).

Hardened cementitious materials comprise tiny pores and cracks, which decrease their lifespan in corrosive environments. Common mechanisms of degradation, including chemical degradation caused by chloride and sulfate ions or freeze-thaw cycles, were found to be related to the transport of external water in the porous network of the cementitious structure (Zhang et al., 2017; Shah et al., 2021; Haq et al., 2022). Thus, various latex admixtures were used to modify cement mortar and concrete in terms of their water permeability. Liu Z. et al. (2023) developed hydroxylated hexagonal boron nitride/isobutyltriethoxysilane hybrid latexes to modify cement composites, decreasing their water absorption coefficient. Wu et al. (2023); Wu et al. (2024) used PAE latex admixture in cement grout which led to the eliminating of macropores and reducing the presence of mesopores and micropores. Zhang et al. (2019) investigated the impact of SAE latex on the mechanical properties and microstructure of various Portland cement mortars, finding that the SAE polymer film adhered the hydration products and filled the pores, thereby reduced water absorption.

Synthetic latexes are produced by emulsion polymerisation, an eco-friendly and efficient technique that generates aqueous dispersion of spherical polymer particles with diameters ranging from 0.05 to 0.50 µm. This process involves free radical polymerisation in an aqueous environment, beginning with the dispersion of monomers in water using an emulsifier, followed by the initiation of polymerisation of the monomers with a water-soluble initiator. The benefit of the emulsion polymerisation technique lies in the design variability of the final polymer particles, which can be easily modified by adjusting the monomer composition, particle size, or cross-link density (Wiley-VCH, 2002; Chern, 2006; Saldívar-Guerra and Vivaldo-Lima, 2013; Machotová et al., 2021). A wide variety of monomers can be used in emulsion polymerisation, most of which are petroleum-based, including styrene, vinyl acetate, and various esters of acrylic and methacrylic acids (Guerrero-Santos et al., 2013). Increasing environmental concerns and the finite nature of fossil resources were prompted research into new materials and strategies aimed at sustainable development, ultimately reducing the environmental impact (Lathi and Mattiasson, 2007; Yao and Tang, 2013; Biswas and Roy, 2015; Laurentino et al., 2018; Allasia et al., 2022). Among these research efforts, vegetable oils were proposed as a suitable alternative to fossil fuels due to their sustainability and abundance (Mecking, 2004; Ragauskas et al., 2006; Williams and Hillmyer, 2008). They consist of triglycerides of higher fatty acids and vary in their degree of unsaturation (Teramoto, 2011; Quirino et al., 2015). However, the double bonds in their molecules are not reactive enough to be used successfully in emulsion polymerisation, so they must be modified by introducing more reactive groups. Epoxidation and subsequent acrylation are two possible approaches (Ferreira et al., 2015; Moreno et al., 2015). Many vegetable oils were utilised in polymer synthesis, including soybean (Wu and Li, 2018), rapeseed (Ho et al., 2022), linseed (Wuzella et al., 2012), or camelina oil (Balanuca et al., 2015). However, the use of vegetable oil-based monomers in emulsion polymerisation remains a challenge due to their natural hydrophobicity, although successful attempts have been reported (Bunker and Wool, 2002; Delatte et al., 2014; Demchuk et al., 2016; Neves et al., 2018).

In our previous papers (Kolář et al., 2023b; Kolář et al., 2023a), a synthesis of acrylated vegetable oil-based monomers from various vegetable oils and their successful copolymerization with standard petroleum-based acrylic monomers via emulsion polymerisation, yielding partially vegetable oil-based film-forming latexes, were demonstrated. The increased water resistance of the resulting coating films with vegetable oil-based monomer contents ranging from 20 to 30 wt% was observed, which motivated this work. The presented paper, therefore, deals with partially vegetable oil-based film-forming latexes (vegetable oil-based monomer/petroleum-based monomers in the weight ratio of 30/70) and their application as cement admixtures to improve the properties of Portland cement mortars. The effect of copolymerized vegetable oil-based monomer type (given by the nature of the vegetable oil, namely, camelina, linseed, and rapeseed oil) on cementitious materials' physical, chemical, mechanical, and water transport properties was evaluated and compared.

# 2 Materials and methods

#### 2.1 Materials

Partially vegetable oil-based latexes were synthesised from (i) petroleum-based monomers, specifically, methyl methacrylate (MMA, Sigma-Aldrich, Schnelldorf, Germany), butyl acrylate (BA, Synthomer, Sokolov, Czech Republic), and methacrylic acid (MAA, Sigma-Aldrich, Schnelldorf, Germany); (ii) laboratory-synthesised vegetable oil-based monomers; (iii) emulsifier, specifically, Disponil FES 993 (BASF, Prague, Czech Republic); (iv) initiator, namely, ammonium persulfate (Lach-Ner, Brno, Czech Republic). 2-Amino-2-methyl-1-propanol (AMP 95, Sigma-Aldrich, Schnelldorf, Germany) was used for neutralising the latex. Vegetable oilbased monomers were synthesized from the following materials: linseed oil (V\_LO, Hb-Lak, Ústí nad Labem, Czech Republic), camelina oil (V\_CO, The National Agricultural and Food Center, Pstruša, Slovakia), rapeseed oil (V\_RO, Preol, Lovosice, Czech Republic), hydrogen peroxide (30%, technical grade, Lach-Ner, Brno, Czech Republic), potassium hydroxide (Lach-Ner, Brno, Czech Republic), potassium carbonate (Lach-Ner, Brno, Czech Republic), methanol (Penta, Prague, Czech Republic), formic acid (Penta, Prague, Czech Republic), hydroquinone (Penta, Prague, Czech Republic), ethyl acetate (Lach-Ner, Brno, Czech Republic), and sodium carbonate (Lach-Ner, Brno, Czech Republic), acrylic acid (Sigma-Aldrich, Schnelldorf, Germany), chromium (III) 2ethyl hexanoate (ThermoFisher, Kandel, Germany). All chemicals were used as obtained.

The cement composite specimens were prepared using the ordinary Portland cement 42.5 R grade (CEM I), produced by Heidelberg Materials CZ, Corp., Czech Republic, and meeting the requirements specified in EN 197-1 (2013). The chemical composition and physical properties of CEM I are given in our previous study (Zárybnická et al., 2023). As a filling material, a natural silica aggregate mixture (SAM, Filtrační písky, Ltd., Czech Republic), composed of three fractions (0.0/0.5 mm, 0.5/1.0 mm, and 1.0/2.0 mm) and mixed in equal weight ratios, was used.

# 2.2 Preparation and characterisation of latex admixtures

First, the vegetable oil-based monomers with the chemical character of methyl esters of acrylated higher fatty acids derived from the respective vegetable oil V\_CO, V\_LO, and V\_RO (see Figure 1a) were synthesised using procedures described in detail in references (Kolář et al., 2023b; Kolář et al., 2023a). In a simplified way, the synthesis of vegetable oil-based monomers was performed according to a 3-step procedure: (i) transesterification of vegetable oil (210 g) using methanol (46 g) and potassium hydroxide (1.85 g) as a catalyst at 60 °C for 90 min; (ii) epoxidation of the transesterification intermediate (210 g) using hydrogen peroxide (172.5 g) and formic acid (30.15 g) as a catalyst at 60 °C for 3 h (potassium carbonate was used to stop the reaction); (iii) acrylation of epoxidized intermediate (50 g) using acrylic acid (17 g), chromium (III) 2-ethyl hexanoate (0.5 g) as a catalyst, and hydroquinone (0.15 g) as an inhibitor (of acrylic acid homopolymerization) at 100 °C for 6 h. Sodium bicarbonate was used to neutralise the excess amount of acrylic acid, and a mixture of ethyl acetate with water (1:1 w/w) and sodium carbonate was utilised for the purification and desiccation of the final product, respectively. A detailed procedure of the synthesis pathway leading to vegetable oil-based monomers is presented in the Supplementary Material.

A semi-continuous, non-seeded emulsion polymerisation technique was employed to synthesise three partially vegetable oil-based latex admixtures, labelled CO, LO, and RO (reflecting the vegetable oil type V\_CO, V\_LO, and V\_RO, respectively). In these latexes, the respective vegetable oil-based monomer (30 wt% in the total monomer mixture) was copolymerized with commercial petroleum-based monomers MMA, BA, and MAA (see Table 1). A reference latex (REF) was also synthetised without introducing a vegetable oil-based monomer. The monomer composition of all synthesized latexes maintained a constant MMA/BA ratio of 21/28 (w/w) to ensure film-formation of latex films at usual ambient temperatures (using the Fox equation (Fox and Flory, 1950), the glass transition temperature  $(T_g)$  was calculated to be approximately 0 °C for the MMA/BA/MAA (42/56/2 by weight) reference copolymer) and also to show the plasticizing effect of the vegetable oil-based monomer type. In all latex compositions, a constant content (2 wt%) of MAA was introduced to provide colloidal stability to the latexes through carboxyl functionalities. A schematic structure of a latex copolymer is shown in Figure 1b.

The latexes were synthesised in a 500 mL glass vessel at 85 °C under a nitrogen atmosphere. 32.5 g of demineralised water, 0.25 g of Disponil FES 993, and 0.35 g of ammonium persulfate were weighed into the glass vessel and heated to the polymerisation temperature. The monomer emulsion consisting of 100 g of the monomer mixture (Table 1), 115 g of demineralised water, 7.4 g of Disponil FES 993, and 0.7 g of ammonium persulfate was then dosed into the reactor during 2 h. After that, the reaction mixture was allowed to polymerise for 2 h. After cooling, the latex was filtered to remove the coagulum formed during the synthesis. Finally, the pH of the latex was adjusted to 10 using AMP 95 (50% aqueous solution). The reaction flow chart graphically summarizing individual synthesis steps of latex nanodisperisons (including vegetable oil-based monomer synthesis) is shown in the Supplementary Material as Supplementary Figure S1.

The solid content was determined according to EN 3251 (2003). The test details are described in detail in the Supplementary Material. The apparent viscosity was measured at 25 °C using a Brookfield LVDV-E Viscometer (Brookfield Engineering Laboratories, USA) at 100 rpm according to the standard EN 2555 (2018). The average particle size (hydrodynamic diameter) and the zeta potential of the latex particles dispersed in water were detected at 25 °C by dynamic light scattering (DLS) using a Litesizer 500 instrument (Anton Paar, Austria). The concentration of a solid polymer in the water phase was 0.01 wt% in all DLS measurements. The minimum film-forming temperature (MFFT) was measured according to the standard ISO 2115 (1996) using an MFFT-60 instrument (Rhopoint Instruments, UK). The testing of colloidal stability against alkaline pH and CaCl2 electrolyte (i.e., ionic strength) was carried out by dropping a small amount (2–3 drops) of the latex into a NaOH solution of a specific pH (10.5, 11.0, 11.5, 12.0, 12.5, 13.0, 13.5, and 14.0) and CaCl<sub>2</sub> solution of a particular concentration (1.0, 1.5, 2.0, 2.5, and 3.0 wt%), respectively.

Schematic structures, (a) vegetable oil-based monomer represented by methyl ester of acrylated oleic acid, (b) copolymer chain composed of MMA

(n), BA (o), MAA (p), and vegetable oil-based monomer (q) represented by methyl ester of acrylated oleic acid.

TABLE 1 Monomeric composition of latex polymer admixtures.

Latex name Vegetable oil-based monomer/wt?	oil-based	Petroleum-based monomer/wt%					
	monomer/wc/	MMA	ВА	MAA			
REF	0	42.00	56.00	2.00			
X <sup>a</sup>	30	29.16	38.84	2.00			

 $^{\mathrm{a}}\mathrm{X}$  is CO, LO, and RO, which reflect the type of vegetable oil (V\_CO, V\_LO, and V\_RO, respectively).

If there was no precipitation, the latex was considered stable at the given pH or CaCl<sub>2</sub> concentration.

Free-standing films with a thickness of approximately 0.7 mm were prepared by pouring the latexes into silicone molds to determine the dry latex polymer's chemical composition,  $T_{\rm g}$ , gel content, and cross-link density. The films were dried at ambient temperature (22 °C ± 1 °C) for 1 month. The chemical composition was characterized by Fourier transform infrared spectroscopy (FTIR). Infrared (IR) spectra were recorded on a Nicolet iS50 FTIR spectrometer (Thermo Fisher Scientific, Waltham, MA, United States), equipped with a built-in diamond attenuated total reflection (ATR) crystal, in the region of 4,000–400 cm $^{-1}$  (data spacing = 0.5 cm $^{-1}$ ). The  $T_{\rm g}$  was determined by differential

scanning calorimetry (DSC) on a Pyris 1 DSC instrument (Perkin-Elmer, Waltham, MA, United States). The measurements were performed under an inert (nitrogen) atmosphere at a heating rate of  $10~{\rm ^{\circ}C \cdot min^{-1}}$  from  $-50~{\rm ^{\circ}C}$  to  $120~{\rm ^{\circ}C}$ , and the  $T_{\rm g}$  value was determined from the second heating curve.

The gel content was determined according to EN 6427 (2014). Approximately 1 g of a dried polymer film was extracted in tetrahydrofuran for 24 h using a Soxhlet extractor.

The cross-link density, expressed as moles of cross-links per cm³ of a polymer network, was determined through swelling experiments on dry latex film specimens (approximately 0.3 g) submerged in toluene at 40 °C for 14 days. The calculations using a set of equations (Vandenburg et al., 1999) based on the Flory and Rehner (1943) are described in more detail in the Supplementary Material. Calculations were performed for the MMA/BA/MAA (42/56/2 by weight) copolymer using density and solubility parameter literature data for poly (MMA), poly (BA), and poly (MAA) homopolymers (Vandenburg et al., 1999; Tobing and Klein, 2001).

# 2.3 Preparation and characterization of portland cement mortars

The mixing ratios of the components used to produce the reference mortar mix (OPC) and the latex-modified mortar mixes

TABLE 2 Proportions of components for the preparation of OPC and cement composite mortar mixes.

Material	Composition/kg m <sup>-3</sup>				
	OPC	CM_ REF	CM_ CO	CM_ LO	CM_ RO
CEM I	500.0	500.0	500.0	500.0	500.0
SAM	1,500.0	1,500.0	1,500.0	1,500.0	1,500.0
Latex	0	0.5	0.5	0.5	0.5
Water	250.0	249.7	249.7	249.7	249.7

are shown in Table 2. The mortar specimens are designated OPC and CM\_y, where y denotes the latex type (REF, CO, LO, and RO). The standard OPC mix consisted of Portland cement, SAM, and water, with a weight ratio of these components of 1.0:3.0:0.5. The influence of latex admixture was investigated in a series of mortars, where a specific latex admixture was added at a level of 0.1 wt% based on the weight of the Portland cement. After mixing the latex admixture with water, the resulting aqueous phase was combined with the remaining mortar composition. The same water-to-cement (w/c) ratio of 0.5 was maintained in all the mortar mixes prepared to ensure the materials were comparable. It is essential to note that the water contained in the latex admixture was subtracted from the initial water added to the batch in the case of the latex-based mortars. According to EN 196-6 (2010), a laboratory mixer that meets all requirements was used to prepare fine OPC and latex-modified mortars. Specimens in the shape of prisms with sizes of  $40 \times 40$ × 160 mm<sup>3</sup> from fresh OPC and latex-modified mortars were cast. The casting and curing processes are described in detail elsewhere (Pokorný et al., 2021a). The prepared hardened mortar specimens were immersed in water for 24 h, as recommended, to prevent elution of the polymer from the cement matrix (Ferreira et al., 2015). At least 18 replicates were casted for each mix.

Isothermal conduction calorimetry (ICC) using a TAM-Air (TA Instruments, Germany) was employed to track the heat signal during the setting reaction of powder and liquid starting components of the same composition, as reported in Table 2. Specimens were equilibrated at a measurement temperature of 25 °C, the slurry was mixed for 120 s, and heat flow was recorded over 7 days. A minimum of two replicates was used. The spread values of the produced specimens were measured following the recommendations described in EN 1015-3 (2000).

Following the 28-day hardening period, a series of analyses were conducted on the produced specimens, as described in the following text. X-ray powder diffraction (XRPD) patterns were collected with a Bragg–Brentano  $\theta$ - $\theta$  diffractometer [Bruker D8 Advance, United States, Cu K $\alpha$  radiation ( $\lambda$  = 1.5418 Å)] at 40 kV and 40 mA in the angular range 5°–60°. 2 $\theta$  counting was set to 0.4 s for each step of 0.0102°. Quantitative phase analysis (QPA) was conducted using the TOPAS 4.2 software (Bruker AXS) with Rietveld refinement. The amorphous phase was quantified using an internal standard method, with zinc oxide added to the specimens at a concentration of 10 wt%.

The microstructures of the specimens were observed using scanning electron microscopy (SEM) with a Quanta 450 FEG (FEI, Czech Republic) and a secondary electron detector. An acceleration voltage of 20 kV was used to observe the 10 nm gold-coated fracture surfaces. The pore size distribution was measured using mercury intrusion porosimetry (MIP) using an Autopore IV 9500 (Micrometrics, United States). Ultrasonic pulse velocity (UPV) and transit time were measured using a Pundit Lab device (Proceq, Switzerland) with a frequency of 250 kHz. The measuring uncertainty was 1.8°%. The flexural and compressive strengths were determined and calculated according to the methodology outlined in EN 1015-11 (1999), using a hydraulic press Servo Plus Evolution (Matest, S.p.A., Italy) with loading capacity up to 300 kN. The expanded combined uncertainty of strength properties assessment was in maximum 2.2%. Water transport measurements of vertical suction were conducted following the procedure outlined in the standard EN 1015-18 (2003). The exact description of liquid transport measurements is provided elsewhere (Pokorný et al., 2021b; Zárybnická et al., 2023). The combined uncertainty of the absorption coefficient  $(kg \cdot m^{-2} \cdot s^{-1/2})$  and apparent moisture diffusivity  $(m^2 \cdot s^{-1})$  did not exceed 10.0%.

## 3 Results and discussion

# 3.1 Vegetable oil-based latex characterization

The characteristic properties of the prepared liquid latex admixtures are listed in Table 3. The solids content of all partially vegetable oil-based latex admixtures was lower than the solids content of the REF latex, which is a result of the increased coagulum formation during the synthesis of the partially vegetable oilbased latexes; 4.5-5.6 wt% of the coagulum (based on total solids) was formed when synthesizing the vegetable oil-based latexes, whereas approximately 0.1 wt% of the coagulum was collected after the synthesis of the REF latex. All latex admixtures exhibited low viscosities, suggesting favorable application and processing properties. The diameters of polymer particles were found not to be affected significantly by the type of vegetable oil-based monomer. They reached values typical for latex polymer products used in building industry applications (Scrivener et al., 2019). On the contrary, the zeta potentials were shown to be affected pronouncedly by the vegetable oil-based monomer used. The zeta potential, which is the electric potential at the boundary of the double layer surrounding the colloidal particle, represents the degree of electrostatic stabilization by repulsive forces between ionically charged colloidal particles. The REF latex admixture showed the lowest zeta potential (in absolute value), suggesting decreased colloidal stability. In contrast, the vegetable oil-based latexes exhibited higher zeta potential values, indicating stability even in harsher conditions (e.g., increased ionic strength, which can occur in the environment of mortar mixes). The MFFT values of all latex admixtures were found to be near or below 0 °C, which suggests the favorable adhesion and binding capability of latex polymer particles among mortar constituents, even at low application temperatures (Zarybnicka et al., 2021).

TABLE 3 Characteristic properties of liquid latex admixtures.

Specimen	Solids content /wt%	Viscosity/mPa <sup>·</sup> s	Particle diameter /nm	Zeta potential/mV	MFFT /°C
REF	39.2 ± 0.1	11.1 ± 0.1	90.2 ± 1.4	-29.2 ± 1.3	0.7 ± 0.2
СО	$37.2 \pm 0.1$	$14.8 \pm 0.2$	$95.0 \pm 0.7$	$-36.7 \pm 2.4$	<0
LO	$36.9 \pm 0.2$	$16.0 \pm 0.2$	92.2 ± 1.1	$-34.3 \pm 1.6$	<0
RO	$37.0 \pm 0.3$	$10.6 \pm 0.1$	90.98 ± 1.5	$-40.9 \pm 2.0$	<0

The testing of colloidal stability against alkaline pH revealed that all latex admixtures remained stable up to pH = 13.5 (see Table 4). Since the pH of the Portland cement mortar environment is below 14 (Sumra et al., 2020), the risk of destabilization (premature aggregation of polymer particles) due to increased pH may be eliminated for all latex admixtures in the preparation process of cement composites. The testing of colloidal stability against CaCl2 electrolyte revealed differences between the latex admixtures (see Table 4). In accordance with the results of zeta potential measurements, the REF latex was found to be the least stable (coagulation occurred at a CaCl2 electrolyte concentration of 1.5 wt%), whereas the vegetable oil-based latexes withstood even the highest tested CaCl<sub>2</sub> electrolyte concentration (3.0 wt%). This fact indicates stronger adsorption of the utilized anionic emulsifier to polymer particles in the vegetable oil-based latex formulations, which may result in decreased/slower/gradual desorption of emulsifier molecules in aqueous solutions of electrolytes at higher concentrations, e.g., in a fresh-mixed mortar environment. Note that adsorbed ionic emulsifier molecules typically represent a significant amount of charge on the surface of polymer particles, thus providing their sufficient electrostatic repulsion (Hellgren et al., 1999). In addition, the increased electrolyte stability of the vegetable oil-based latex admixtures can also prevent premature aggregation (flocculation) of latex polymer particles in the intended mortar application, which should result in increased/uniform distribution of latex polymer in the cement composite and its higher binding ability.

The prepared latex admixtures were also investigated from the point of view of their chemical structure and the level of cross-linking expressed by the parameters of gel content and cross-link density (see Table 5). The chemical structure of latex admixtures in terms of the vegetable oil incorporation was characterized by FTIR spectroscopy. The IR spectra of the vegetable oil-based latex admixtures (Figure 2) exhibit increased intensity of the C–H stretching bands of the methylene groups at 2,933 and 2,857 cm $^{-1}$  ( $\nu_a$  (C–H; CH $_2$  and  $\nu_s$  (C–H); CH $_2$ , respectively), which documents the successful incorporation of the vegetable oil-based monomers into the acrylic polymer chains.

Cross-linking of latex polymers may affect their applicability and final properties, e.g., mechanical and chemical resistance may be improved due to toughening of the polymer structure. However, on the other hand, adhesion and coalescence can deteriorate due to loss of polymer particle deformability (Machotova et al., 2016). In our previous works on the synthesis of vegetable oil-based latexes for coating applications (Kolář et al., 2023a; Kolář et al., 2023b), it

TABLE 4 Results of colloidal stability tests of liquid latex admixtures against alkaline pH and CaCl<sub>2</sub> electrolyte.

Specimen	Alkaline pH stability <sup>a</sup> pH/-		CaCl <sub>2</sub> electrolyte stability CaCl <sub>2</sub> concentration/wt%				
	13.5	14	1.0	1.5	2.0	2.5	3.0
REF	√	_	1	-	-	-	-
СО	√	_	1	√	√	√	√
LO	√	_	1	√	√	√	√
RO	√	_	√	√	√	√	√

<sup>a</sup>Stability results are presented by symbols: "\"\" means no visible coagulation or no visible precipitation of latex in test solution; "\"\" means visible coagulation or precipitation of latex in test solution.

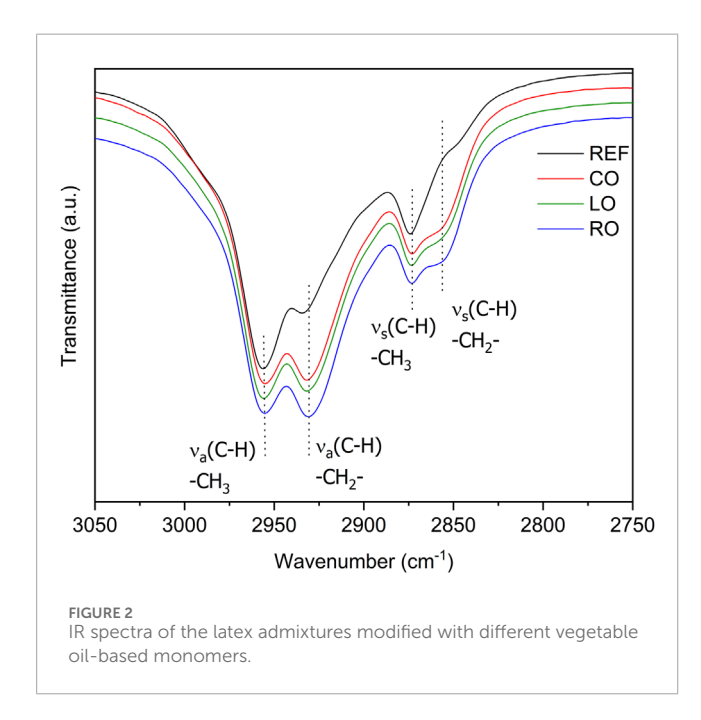
was demonstrated that cross-linking occurred within the individual latex polymer particles due to copolymerizing the vegetable oil-based monomers containing multi-acrylated ingredients derived from polyunsaturated higher fatty acids (the detailed representation of higher fatty acids in utilized vegetable oils is provided in Supplementary Table S1 in the Supplementary Material). This phenomenon was also confirmed in this study, showing the significant amount of gel fraction and measurable values of cross-link density for all partially vegetable oil-based latex polymers, among which the LO polymer exhibited the highest level of cross-linking and the RO polymer was the least cross-linked, suggesting the most favorable sintering and adhesion of the RO latex admixture to mineral parts of the mortar.

The prepared latex admixtures were also investigated from the point of view of polymer  $T_{\rm g}$  (see Table 5). This parameter expresses the mobility of polymer chains. It is also related to the deformability, adhesion, and binding capability of spherical latex polymer particles to mineral components of the mortar, thus affecting the cohesion and mechanical performance of the final cement composite material. It was found that the vegetable oil-based latex polymers exhibited lower  $T_{\rm g}$  values in comparison with the REF latex polymer. A significantly reduced  $T_{\rm g}$  was found for the RO latex polymer, indicating increased deformability of the polymer particles and better adhesive and bonding ability of the RO latex admixture.

TABLE 5 Characteristic properties of dry latex polymers.

Specimen	Gel content/wt%	Cross-link density $\times$ $10^{-6}$ /moles of cross-links $\times$ cm $^{-3}$	Τ <sub>g</sub> /°C
REF	_a	≅ 0	1.3 ± 1.0
СО	86.8 ± 0.5	227 ± 8	$-2.0 \pm 0.5$
LO	90.9 ± 1.2	$399 \pm 10$	$-1.8 \pm 0.9$
RO	$72.0 \pm 0.9$	32 ± 1	-13.4 ± 1.2

<sup>&</sup>lt;sup>a</sup>The gel fraction was not present.



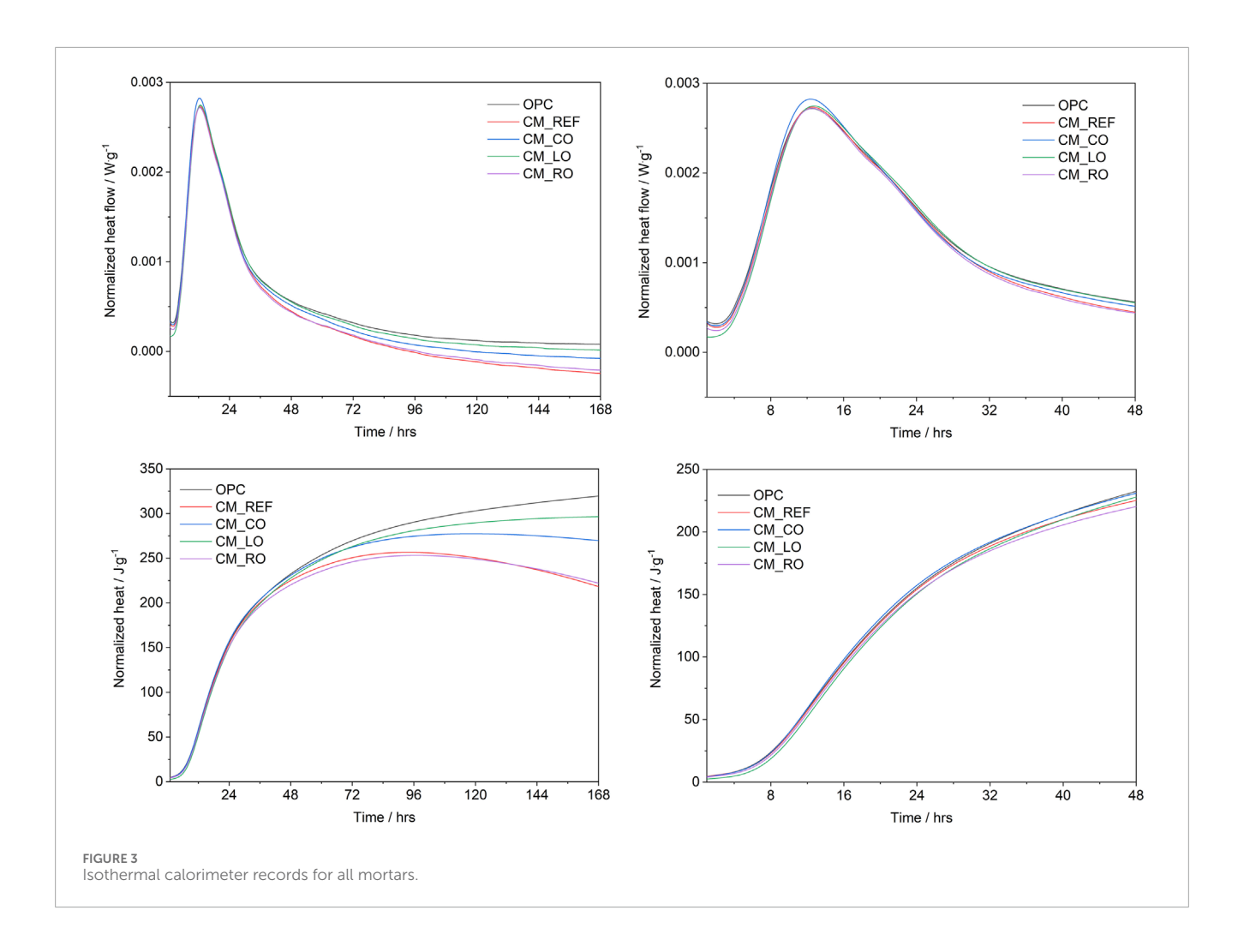
# 3.2 Monitoring of the hydration process of portland cement mortars

The recorded heat and heat flow curves are depicted in Figure 3. The pre-induction phase is not reported as it was of a relatively brief duration (approximately 10-15 min), and this period is solely represented by the wetting of the cement grains. Subsequently, the initial reactions with the clinker minerals occurred. A quantity of hydration heat was released, accompanied by the dissolution of aluminates and sulfates and the formation of portlandite [CH, Ca(OH)<sub>2</sub>] (Lothenbach and Winnefeld, 2006). A comparison of the measured records indicates that the behavior of all types of mortars is comparable. The next phase is distinguished by a gradual release of hydration heat, an increase in viscosity (indicative of the beginning of cement solidification), and the formation of nuclei for calcium silicate hydrate (C-S-H) and CH crystals (Beaudoin and Odler, 2019). The formation of ettringite (AFt; calcium trisulfoaluminate hydrate) persists, accompanied by the penetration of water into the cement grains and the formation of new hydration products. The second phase of the induction period is completed approximately one to 2 hours after mixing. Then, the rate of hydration was increased, with the maximum at around 12 h. During this cement hydration phase, the individual mortars' behavior remained comparable, with a slightly higher curve for the CM\_CO mortar.

The next step is characterized by the rapid reaction of Alite (C<sub>3</sub>S, tricalcium silicate) and formation of long-fiber silicate C-S-H and CH crystals. The cement grains are approached by each other because of the growth of crystals of hydration products (Scrivener et al., 2019). During this period, the fundamental structures of cement are established (Brown et al., 1984). The finefiber C-S-H is formed in the following phase of the hydration process, and AFt gradually transforms into monosulfate (AFm), belite (C2S) undergoes hydration, and the generation of heat decreases. Diffusion then controls the hydration reactions. After approximately 30 h of hydration, a distinct change in heat flow curves was observed in the CM\_RO and CM\_REF mortars, characterized by reduced heat generation. The process of hydration of the CM\_CO, CM\_LO, and OPC mortars was comparable up to 48 h, after which a decrease in heat generation was observed compared to OPC. The total heat of hydration was measured after 7 days, with the highest values determined for OPC (339 J·g<sup>-1</sup>), CM\_LO (297.5 J·g<sup>-1</sup>), and CM\_CO (277.4) J·g<sup>-1</sup>. The lowest values were calculated for CM\_RO (253.2  $J \cdot g^{-1}$ ) and CM\_REF (256.7  $J \cdot g^{-1}$ ). Concerning the testing of mechanical properties, it was found that the mortars with the highest total heat demonstrated the optimal performance, a finding substantiated in the following text. The shape and progress of detected heat and heat flow curves of cement hydration processes, as well as total heat, were found to be comparable with previously described isocalorimetric measurements of cement composites produced using different types of admixtures like e.g., acrylic latexes (Zárybnická et al., 2023; Machotová et al., 2025) and/or latex copolymer of carboxylate styrene-butadiene (Baueregger et al., 2015).

# 3.3 Mineralogical composition of hardened portland cement mortars

From a qualitative point of view, quartz (Si, SiO<sub>2</sub>), CH, calcite (CC, CaCO<sub>3</sub>) together with its metastable polymorphs – aragonite and vaterite (both CaCO<sub>3</sub>), gypsum (CSH<sub>2</sub>, CaSO<sub>4</sub>.2H<sub>2</sub>O), unreacted clinker phases (C<sub>3</sub>S, C<sub>2</sub>S) and Aft, the product of the reaction between C<sub>3</sub>S and CSH<sub>2</sub> during cement hydration, were detected. The quantitative mineralogical analysis of the collected



XRPD patterns, including quantification of the amorphous phase, is summarized in Table 6.

In contrast to our previous works focused solely on the petroleum based polymeric admixtures (Zárybnická et al., 2023; Machotová et al., 2025), no or only a negligible amount of vaterite phase was detected in hardened CM specimens, probably as a consequence of the modification of hydration and/or carbonation pathways due to the effects of the different chemical nature of applied latexes. Generally, the presence of CaCO<sub>3</sub> may be explained by the partial release of Ca<sup>2+</sup> ions from amorphous C-S-H phases (Sevelsted and Skibsted, 2015) or due to the carbonation reaction (Liang et al., 2024). To highlight the effects of incorporated vegetable oil-based derivatives in latexes, the results of the quantitative phase analysis were recalculated, excluding quartz that was detected in the specimens due to the used aggregate fraction, and the graphical output is visualized in Figure 4.

As visible in Figure 4, the significant difference between vegetable oil-based latex mortar specimens and OPC and CM\_REF specimens was found to be in the amount of CaCO<sub>3</sub> and amorphous phases. Compared to CM\_REF, specimens containing vegetable oil-based latex admixtures with linseed (CM\_LO) and, especially, rapeseed oil (CM\_RO) showed lower concentrations of CaCO<sub>3</sub> and higher amounts of amorphous phase – assumed to be mainly composed of C-S-H (Bullard et al., 2011). On

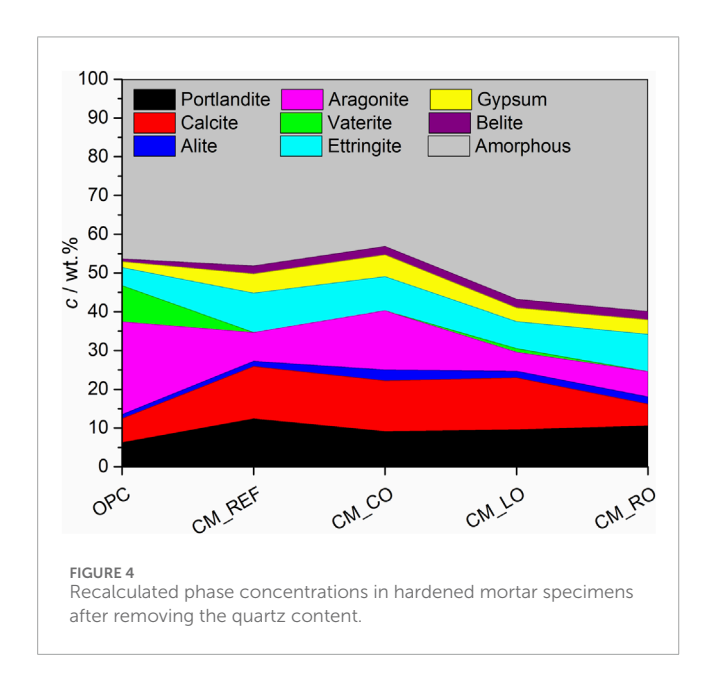
the contrary, the opposite trend was detected for specimens with the vegetable oil-based latex admixture containing camelina oil (CM\_CO). The tremendous effects of various admixtures and admixtures on the reaction kinetics and pathways of both hydration and carbonation reactions in cementitious and lime-based systems are well documented (Cheung et al., 2011; Rodriguez-Navarro et al., 2023).

# 3.4 Microstructure of hardened portland cement mortars

The gallery of SEM micrographs collected on fractured mortar specimens is depicted in Figure 5. All specimens have shown well-compacted dense internal microstructure, including OPC, which was already reported in our previous work (Zárybnická et al., 2023). In Figure 5a, long needle-like AFt crystals (Tosun and Baradan, 2010) attached to hydrated clinker phases are visible. As reported in the work on petroleum-based acrylic latexes (Ševčík et al., 2023; Zárybnická et al., 2023), also the partially vegetable oil-based latexes exhibited sufficient bridging capability, for example, the bridge between the cement matrix and silica aggregate is depicted in Figure 5b (area highlighted by the inserted arrow) and in Figure 5e, in which the exact location (delaminated in a white rectangle) is

TABLE 6 The mineralogical composition of selected 28-day hardened mortars as determined using Rietveld refinement.

Phase	Content/wt%				
	OPC	CM_REF	CM_CO	CM_LO	CM_RO
Quartz (S)	42.2 (4)	55.4 (5)	68.1 (5)	45.7 (4)	57.4 (4)
Portlandite (CH)	3.6 (1)	5.5 (1)	2.9 (1)	5.2 (9)	4.5 (1)
Calcite (CC)	3.6 (3)	6.0 (3)	4.2 (3)	7.3 (3)	2.4 (2)
Alite (C <sub>3</sub> S)	0.6 (2)	0.6 (2)	0.9 (2)	0.9 (2)	0.8 (2)
Aragonite	13.9 (3)	3.3 (4)	4.9 (5)	2.7 (3)	2.8 (3)
Vaterite	5.4 (3)	-	-	0.5 (2)	-
Ettringite (Aft)	2.7 (3)	4.5 (3)	2.8 (3)	3.8 (3)	4.1 (3)
Gypsum (CSH <sub>2</sub> )	0.9 (2)	2.2 (2)	1.8 (2)	1.9 (2)	1.6 (2)
Belite (C <sub>2</sub> S)	0.4 (1)	0.9 (2)	0.7 (3)	1.2 (3)	0.9 (2)
Amorphous	26.9 (9)	21.4 (9)	13.8 (9)	30.9 (8)	25.6 (8)



shown at higher magnification. In CM\_LO, a porous space partially filled with a polymer film was detected (Figure 5c, highlighted by an arrow). Observation at higher magnification (see Figure 5f in which cracks formed due to radiation damage by electron beam are visible inside the area highlighted by a white rectangle) confirmed the presence of latex polymer material. Moreover, in the central part of Figure 5d, C-S-H-phases (Chiang et al., 2014) in close connection with plate-like CH (Cizer et al., 2012) and Aft crystals is well visible.

Unfortunately, the application of latex admixtures in cement mortar and concrete is often associated with a bubble-forming effect, resulting in increased porosity of hardened cementitious materials. This phenomenon was ascribed to the desorption of emulsifiers

from polymer particles, which subsequently entrain air during mortar mixing (Wang and Wang, 2011). Therefore, MIP analysis was performed (see Table 7; Figure 6). All specimens comprising the vegetable oil-based latex admixture, regardless of its type, reported a higher rate of open porosity in comparison with OPC and CM\_REF. Compared with CM\_REF, the porosity was found to be 13.9, 19.0, and 20.4% higher for CM\_CO, CM\_LO, and CM\_ RO, respectively. An increased porosity of hardened latex-based composites is related to the foamy effect of latex admixtures in fresh mixes (Łaźniewska-Piekarczyk, 2013; Zárybnická et al., 2023). In previous works (Zárybnická et al., 2023; Machotová et al., 2025), the increased amount of added petroleum/based admixtures into cement composites resulted in the gradual increase of total porosity and increased pore volumes in all three pores diameters regions: gel pores, capillaries and macropores. As demonstrated in Figure 6, showing a graphical representation of the results of the size pore distribution for all specimens, it can be summarized that the CM\_ LO and CM\_RO specimens exhibited a higher content of capillaries and macropores than the OPC specimen. Conversely, the content of capillaries was lower for the CM\_REF and CM\_CO specimens than for OPC. Gel pores were detected at higher quantities in cement composite specimens comprising the vegetable oil-based latex admixtures, while the OPC and CM\_REF specimens were comparable.

Upon examining the information regarding MIP with the stability testing and zeta potentials of the prepared latex admixtures (Tables 3, 4), it can be assumed that in more stable latexes (the RO latex was found to be the most stable, while the REF latex was the least stable) the desorption of the emulsifier from polymer particles in the fresh mortar mix occurred, but more slowly. To draw the following conclusion, these assumptions must be taken into account: (i) the desorbed emulsifier, which in the fresh mortar mix functions as a surfactant (reducing the interfacial tension between liquid and gas), captures air, stabilizes, and also retains air bubbles in the fresh

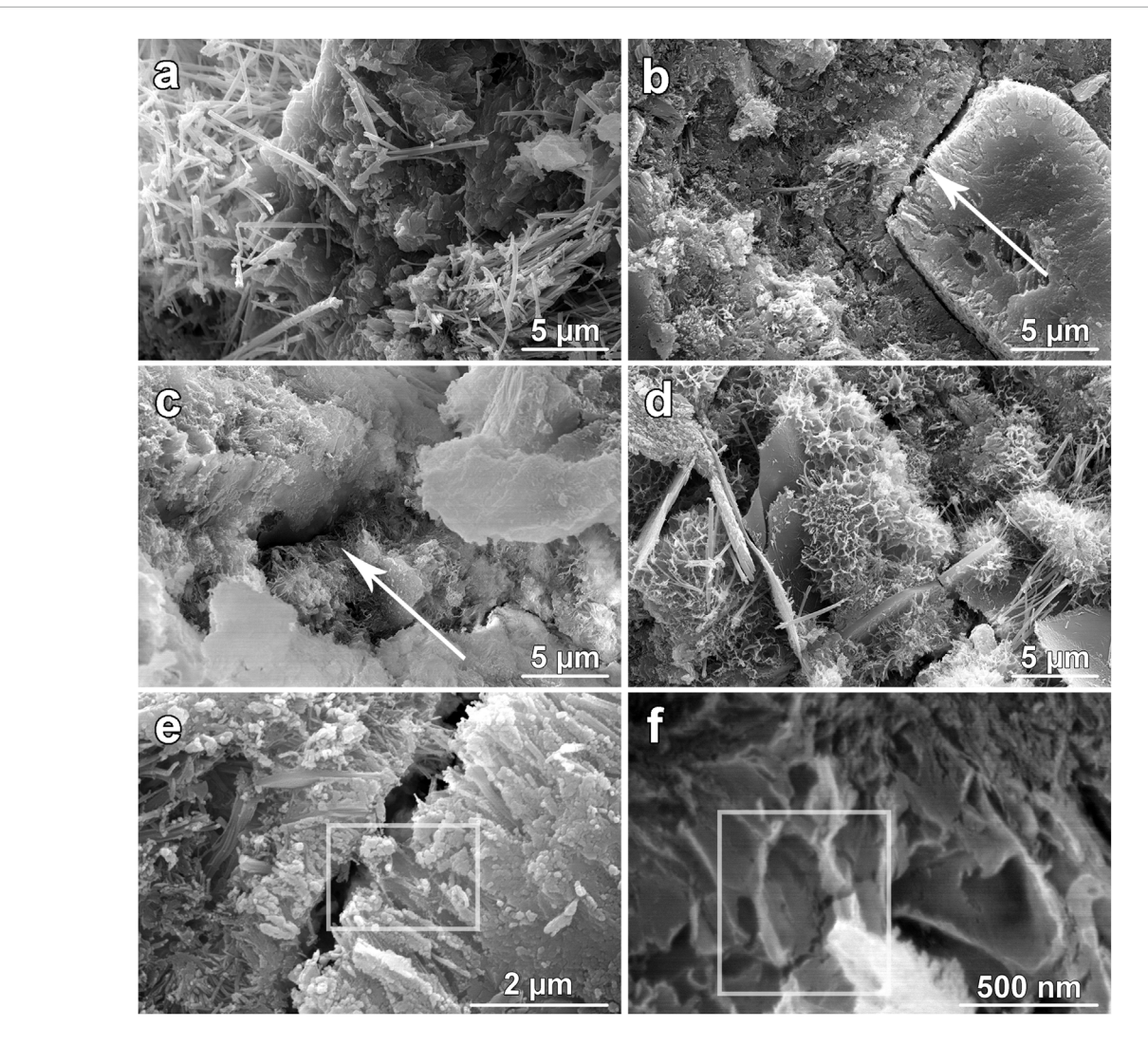


FIGURE 5
Microstructure of 28-day hardened specimens, (a) CM\_REF; (b) CM\_CO; (c) CM\_LO; (d) CM\_RO; (e) detail CM\_CO; (f) detail CM\_LO.

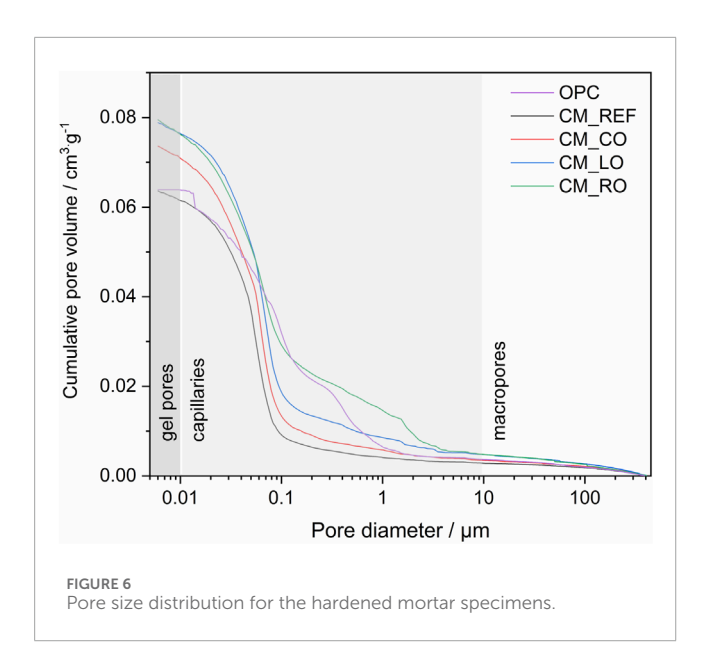
TABLE 7 Porosity (MIP) and ultrasonic characteristics of 28-day hardened OPC and cement composite specimens.

Specimen	MIP/%	Ultrasonic velocity/m <sup>-</sup> s <sup>-1</sup>	Transit time/μS
OPC	13.8	$40.0 \pm 1.5$	4,087 ± 36.8
CM_REF	13.7	$42.2 \pm 0.2$	3,788 ± 13.2
CM_CO	15.6	$42.7 \pm 0.3$	3,750 ± 22.2
CM_LO	16.3	$44.8 \pm 0.5$	3,572 ± 42.1
CM_RO	16.5	$43.9 \pm 0.3$	$3,645 \pm 25.0$

mortar mixture, (ii) large bubbles have a greater chance of escaping from the cement material during the mortar vibrating period. With delayed desorption of the emulsifier, the air present in the mortar mix will still be captured, however, it will probably be present in the form of a higher number of fine bubbles, which, however, will remain trapped in the cement material due to their small size and the advanced stage of mortar hardening.

# 3.5 Physical-mechanical properties of hardened portland cement mortars

Ultrasonic waves are primarily employed to predict the strength of mortar and concrete (Abo-Qudais, 2005), however, this method can also be utilized to identify internal defects, such as cracks (Malhotra and Carino, 2003). It can be assumed that an increase



in transit time and a reduction in ultrasonic velocity result in a more compact structure formation with a lower abundance of internal defects. As reported in Table 7, the most compact specimen appeared to be OPC, which showed the lowest ultrasonic velocity value and, at the same time, the highest transit time value. CM specimens could be sorted into two groups with comparable values represented by CM\_REF and CM\_CO specimens with values of ultrasonic velocity and transition time around 42.3 m·s<sup>-1</sup> and 3,775  $\mu$ S, respectively, and other two specimens (CM\_LO and CM\_RO) with ca. 5% higher velocities values, and, simultaneously, 5% lower transition time values. As discussed in the following text, the ultrasonic characteristics of mortar specimens are closely associated with compressive strength values (Făcăoaru, 1970).

The results of the mechanical characteristics, namely, the compressive and flexural strengths, are listed in Table 8. In the case of compressive strength, produced specimens could be, as in the case of ultrasonic wave tests, divided into 3 groups: (i) the highest compressive strength - OPC, CM\_REF and CM\_CO of; (ii) the moderate compressive strength - CM\_LO; (iii) the lowest compressive strength - CM\_RO. Regarding the vegetable oil-based latex admixture type, negligible differences in compressive strength values were detected for CM\_CO compared to OPC. On the contrary, CM\_LO and, especially, CM\_RO showed lower

compressive strength values (reduction of 15.4% for CM\_RO versus OPC). An explanation of this compressive behavior could be related to the increased porosity of specimens produced using vegetable oil-based latex admixtures, as discussed above. Looking closely at the flexural strength, specimens containing vegetable oil-based latex admixtures showed comparable values with no significant differences. In previous papers (Ismail et al., 2011; Zárybnická et al., 2023), latex concentration was found to play a major role in the flexural strength of cement-based materials, most probably as a consequence of altered air entrapment during the mixing procedure. As possible method to reduce negative impact of the polymeric admixtures on compressive strengths of produced cement composites, a partial substitution of cement with fly ash was proposed (Liu et al., 2020).

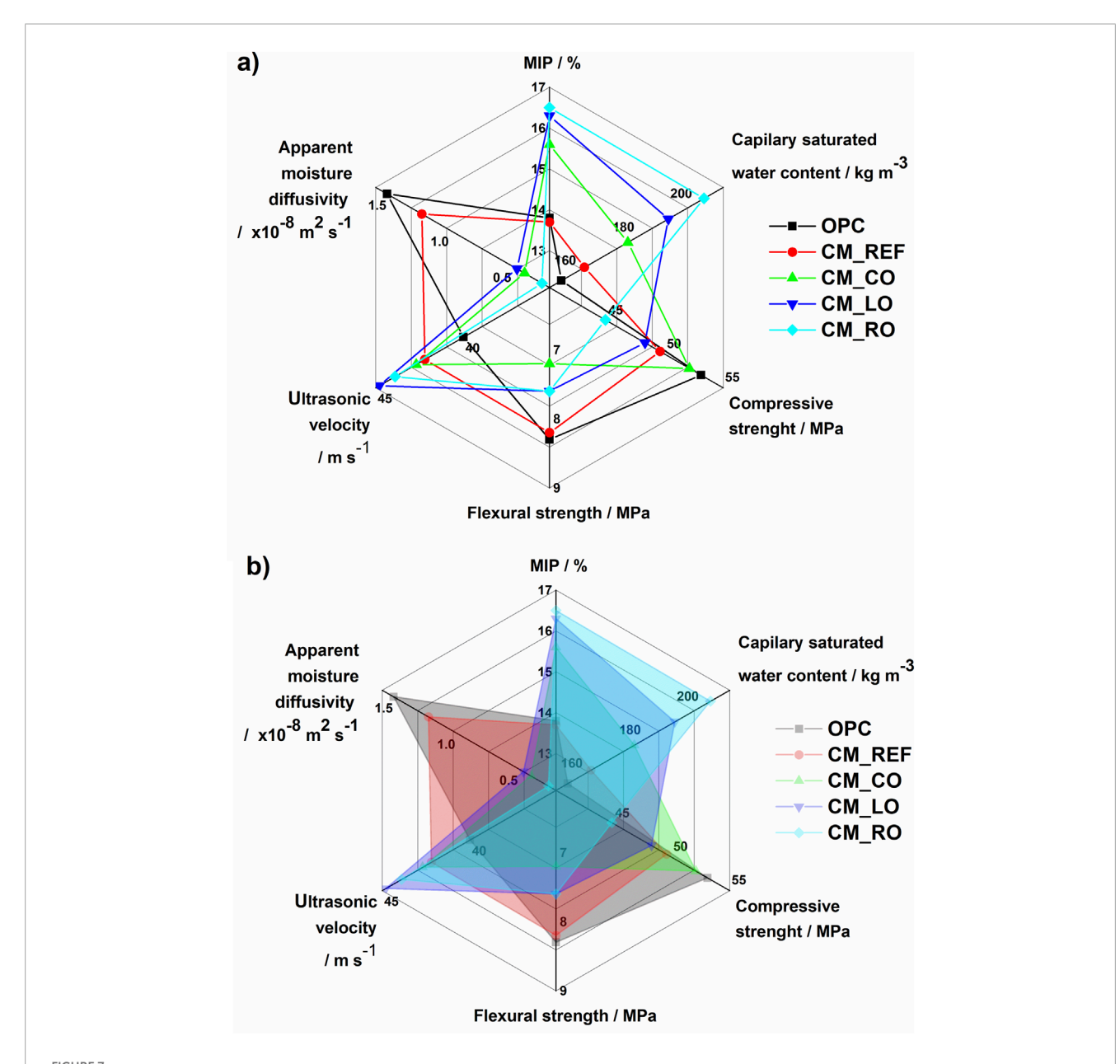
The compactness of the inner structure of hardened mortar specimens is also related to properties that describe the transport of liquid water into the cementitious matrix. In general, water constitutes a suitable solvent medium that allows the penetration of different harmful substances (salts, acids, etc.) into the porous structure of cementitious building materials, causing negative impacts in long-term periods (Luo et al., 2024). The detected characteristics of the liquid water transport results of the produced mortar specimens are summarized in Table 9. The positive effect of vegetable oil-based latex admixtures on mitigating liquid waterrelated transport through the structure of the produced mortars was observed. For example, the positive effect on the permeability of the produced cement composites were observed also for applications of styrene-butadiene rubber latex, polyacrylic ester emulsion and organic silicon waterproof agent (Liu et al., 2020). The intensity of the water suction of mortar specimens indicated by the absorption coefficient values showed the minimal effect of the REF latex admixture - 5.0% (vs. OPC). On the other hand, specimens comprising the vegetable oil-based latexes were found to be very effective in reducing water suction: in contrast to CM\_REF, the absorption coefficient was reduced by 27.8% for CM\_LO and 38.9% for both CM\_CO and CM\_RO, probably as a consequence of their increased effectivity in formation of hydrophobic films inside cement matrix (see Figure 5) that substantially hindered water transport (Knapen and Van Gemert, 2015). The higher porosity of these specimens is responsible for higher capillary saturated water content, but despite that, apparent moisture diffusivity is significantly mitigated from  $1.51 \times 10^{-8}$  (OPC) up to  $0.27 \times 10^{-8}$  $10^{-8} \text{ m}^2 \cdot \text{s}^{-1}$  (CM\_RO). The positive effect of the vegetable oil-based latex admixtures can be attributed mainly to the influence of the

TABLE 8 Mechanical characteristics for 28-day hardened mortar specimens.

Specimen	Compressive strength/MPa	Flexural strength/MPa
OPC	53.1 ± 1.9	$8.3\pm0.2$
CM_REF	49.6 ± 1.4	8.2 ± 0.5
CM_CO	52.1 ± 1.3	7.2 ± 0.7
CM_LO	48.3 ± 0.5	7.6 ± 0.5
CM_RO	44.9 ± 0.6	7.6 ± 0.1

TABLE 9 Liquid water transport characteristics and open porosity of 28-day hardened mortar specimens.

Specimen	Absorption coefficient/kg·m <sup>-2</sup> ·s <sup>-1/2</sup>	Capillary saturated water content/kg·m <sup>-3</sup>	Apparent moisture diffusivity/×10 <sup>-8</sup> m <sup>2</sup> ·s <sup>-1</sup>	Sorptivity/×10 <sup>-5</sup> m⋅s <sup>-1/2</sup>
OPC	0.019	154.2	1.51	1.90
CM_REF	0.018	162.2	1.23	1.18
CM_CO	0.011	177.1	0.41	1.13
CM_LO	0.013	191.1	0.47	1.31
CM_RO	0.011	203.4	0.27	1.05



Comparative radar charts (a) using lines; (b) using area to highlight the changes illustrating the influence of the type of latex admixture on mortar properties.

polymer's  $T_g$  which was significantly lower in the case of the RO latex polymer compared with CO and LO polymers (see Table 5). The low  $T_{\sigma}$  makes latex polymer particles more deformable, enhancing their ability to coalesce and form a continuous, cohesive polymer film within the pores of the cement mortar. This film effectively coats and seals the inner structure, acting as a hydrophobic barrier that lines the pores that would otherwise serve as pathways for water ingress. Moreover, the LO and CO polymer particles exhibited significantly higher levels of internal cross-linking (see Table 5), which made their particles more rigid. The lower level of crosslinking within individual polymer particles of the RO latex enhanced the polymers' flexibility, provided by its low  $T_g$ , further promoting its sintering and adhesion to the mortar constituents. Thus, the RO latex with the lowest  $T_{\rm g}$  and cross-linking level coated and sealed the inner structure of the cementitious material to the greatest extent, resulting in reduced water ingress. These findings suggest the high effectiveness of the newly produced vegetable oil-based latex admixtures, particularly the RO type, in hindering water penetration into the porous structure of mortar and concrete.

Figure 7 and Supplementary Figure S2 Supplementary Material, the radar charts are depicted, illustrating the significant changes in the selected properties of the produced specimens. The close relation of porosity to some properties is visible. For example, the higher porosity values were found to be reflected in the higher values of capillary saturated water content and ultrasonic velocity and lower values of flexural strength. The trends are not so straightforward in the case of compressive strength and, e.g., apparent moisture diffusivity, where the type of the synthesized vegetable oil-based latex admixture considerably influenced the detected values, as already mentioned above. The CO latex admixture seems to be good candidate for the preparation and testing of Portland cement-based mortars intended for structures where high compressive strengths with reduced water transport properties and/or greater durability against weathering (Pang et al., 2025) are needed. In general, water transport properties of the produced mortar specimens were found to be most affected by the application of the RO latex admixture, however, at the cost of the highest decrease in compressive strength. Nevertheless, a decrease in the sorptivity of cementitious materials has been identified as a crucial parameter to predict their lifetime (Tukimat et al., 2017). However, to determine the long-term behavior of produced composites using polymeric bio-based nanodispersed admixtures will need to be comprehensively evaluated, for example, using for accelerated aging tests.

### 4 Conclusion

This work dealt with novel vegetable oil-based latex admixtures synthesized from derivatives of vegetable oils – camelina, linseed, and rapeseed. The role of these bio-based admixtures in modifying chemical, physical, and mechanical properties of Portland cement mortars were investigated. According to the obtained experimental data using a combination of instrumental techniques, the following conclusions were found.

The vegetable oil-based latexes exhibited pH stability up to 13.5 and, compared to the standard latex without the vegetable oil-based component, the better colloidal stability in  $CaCl_2$  electrolyte,

increased cross-link density, and lower glass transition temperatures were detected.

The hydration process of the mortars was found to be significantly affected by the incorporation of the vegetable oil-based latexes after 7 days, with the lowest values of total heat being achieved by specimens CM\_REF and CM\_RO. In contrast, the highest levels of heat development were recorded for the reference specimen OPC.

The application of latex admixtures in mortars resulted in the reduced formation of metastable CaCO<sub>3</sub> polymorphs and, especially in the case of CM\_RO, increased abundance of the amorphous phase.

SEM observations revealed good bridging capability and pores filling capacity of the vegetable oil-based admixtures.

The open porosity of mortar specimens containing vegetable oil-based latex admixtures was found to be around 14%–20% higher, most probably due to increased air entrainment during the mixing procedure.

The increased porosity of mortar specimens with vegetable oil-based latex admixtures was reflected in decreased mechanical performance, except for the CM\_CO specimen, in which compressive strength was found to be comparable to OPC.

Water transport was significantly reduced in the mortar specimens produced with the vegetable oil-based latex admixtures. The absorption coefficient was 30–40% lower versus OPC and CM\_REF. The vegetable oil-based latex admixtures, according to their increased effectivity to alter liquid water transport, could be sorted as RO > CO > LO.

It can be concluded, that bio-based polymeric nanodispersion represents a novel, environmentally friendly, class of cement admixtures that may find utilization in case of structures that are strongly loaded with water and/or water soluble salts.

# Data availability statement

The data that support the findings of this study are openly available in the Figshare repository at <a href="https://figshare.com/s/5cfle2a8fd4c0a1ae335">https://figshare.com/s/5cfle2a8fd4c0a1ae335</a>.

# **Author contributions**

RŠ: Data curation, Formal Analysis, Investigation, Supervision, Visualization, Writing – original draft, Writing – review and editing. MK: Data curation, Investigation, Visualization, Writing – original draft. JP: Data curation, Formal Analysis, Investigation, Resources, Writing – original draft. LZ: Data curation, Formal Analysis, Investigation, Visualization, Writing – original draft. JH: Data curation, Investigation, Visualization, Writing – original draft. JM: Data curation, Funding acquisition, Investigation, Supervision, Visualization, Writing – original draft, Writing – review and editing.

## **Funding**

The author(s) declare that financial support was received for the research and/or publication of this article. This work was

supported by the Ministry of Education of Youth and Sports of the Czech Republic under Grant CZ.02.01.01/00/23\_021/0008593; the Institute of Technology and Business under Grant SVV No. 03SVV2325; and the Czech Academy of Sciences, Institute of Theoretical and Applied Mechanics under Grant RVO 68378297.

#### Conflict of interest

The authors declare that the research was conducted in the absence of any commercial or financial relationships that could be construed as a potential conflict of interest.

#### Generative AI statement

The author(s) declare that no Generative AI was used in the creation of this manuscript.

Any alternative text (alt text) provided alongside figures in this article has been generated by Frontiers with the support of artificial intelligence and reasonable efforts have been made to ensure accuracy, including review by the authors wherever possible. If you identify any issues, please contact us.

### Publisher's note

All claims expressed in this article are solely those of the authors and do not necessarily represent those of their affiliated organizations, or those of the publisher, the editors and the reviewers. Any product that may be evaluated in this article, or claim that may be made by its manufacturer, is not guaranteed or endorsed by the publisher.

# Supplementary material

The Supplementary Material for this article can be found online at: https://www.frontiersin.org/articles/10.3389/fbuil.2025.1701378/full#supplementary-material

## References

Abo-Qudais, S. A. (2005). Effect of concrete mixing parameters on propagation of ultrasonic waves. *Constr. Build. Mater.* 19, 257–263. doi:10.1016/j.conbuildmat.2004.07.022

Ali, U., Shahid, S., and Ali, S. (2021). Combined effects of styrene–butadiene rubber (SBR) latex and recycled aggregates on compressive strength of concrete. *J. Rubber Res.* 24, 107–120. doi:10.1007/s42464-020-00077-1

Allasia, M., Aguirre, M., Gugliotta, L. M., Minari, R. J., and Leiza, J. R. (2022). High biobased content waterborne latexes stabilized with casein. *Prog. Org. Coatings* 168, 106870. doi:10.1016/j.porgcoat.2022.106870

Balanuca, B., Raluca, S., Hanganu, A., Adriana, L., and Iovu, H. (2015). Design of new camelina oil-based hydrophilic monomers for novel polymeric materials. *J. Am. Oil Chem. Soc.* 92, 881–891. doi:10.1007/s11746-015-2654-z

Barbhuiya, S., Kanavaris, F., Ashish, D. K., Tu, W., Das, B. B., and Adak, D. (2025). Ground waste glass as a supplementary cementitious material for concrete: sustainable utilization, material performance and environmental considerations. *J. Sustain. Cem. Mater.* 14, 1221–1249. doi:10.1080/21650373.2025.2493719

Barluenga, G., and Hernández-Olivares, F. (2004). SBR latex modified mortar rheology and mechanical behaviour. *Cem. Concr. Res.* 34, 527–535. doi:10.1016/j.cemconres.2003.09.006

Baueregger, S., Perello, M., and Plank, J. (2015). Influence of carboxylated styrene-butadiene latex copolymer on Portland cement hydration. *Cem. Concr. Compos.* 63, 42–50. doi:10.1016/j.cemconcomp.2015.06.004

Beaudoin, J., and Odler, I. (2019). Hydration, setting and hardening of Portland cement. *Lea's Chem. Cem. Concr.* 5, 157–250. doi:10.1016/b978-0-08-100773-0.00005-8

Betioli, A. M., Gleize, P. J. P., John, V. M., and Pileggi, R. G. (2012). Effect of EVA on the fresh properties of cement paste. *Cem. Concr. Compos.* 34, 255–260. doi:10.1016/j.cemconcomp.2011.10.004

Bilal, H., Chen, T., Ren, M., Gao, X., and Su, A. (2021). Influence of silica fume, metakaolin and SBR latex on strength and durability performance of pervious concrete. *Constr. Build. Mater.* 275, 122124. doi:10.1016/j.conbuildmat.2020.122124

Biswas, A., and Roy, M. (2015). Green products: an exploratory study on the consumer behaviour in emerging economies of the east. *J. Clean. Prod.* 87, 463–468. doi:10.1016/j.jclepro.2014.09.075

Brown, P. W., Franz, E., Frohnsdorff, G., and Taylor, H. F. W. (1984). Analyses of the aqueous phase during early C3S hydration. *Cem. Concr. Res.* 14, 257–262. doi:10.1016/0008-8846(84)90112-1

Bullard, J. W., Jennings, H. M., Livingston, R. A., Nonat, A., Scherer, G. W., Schweitzer, J. S., et al. (2011). Mechanisms of cement hydration. *Cem. Concr. Res.* 41, 1208–1223. doi:10.1016/j.cemconres.2010.09.011

Bunker, S. P., and Wool, R. P. (2002). Synthesis and characterization of monomers and polymers for adhesives from methyl oleate. *J. Polym. Sci. Part A Polym. Chem.* 40, 451–458. doi:10.1002/pola.10130

Chern, C. S. (2006). Emulsion polymerization mechanisms and kinetics. *Prog. Polym.* Sci. 31, 443–486. doi:10.1016/j.progpolymsci.2006.02.001

Cheung, J., Jeknavorian, A., Roberts, L., and Silva, D. (2011). Impact of admixtures on the hydration kinetics of Portland cement. *Cem. Concr. Res.* 41, 1289–1309. doi:10.1016/j.cemconres.2011.03.005

Chiang, W.-S., Ferraro, G., Fratini, E., Ridi, F., Yeh, Y.-Q., Jeng, U. S., et al. (2014). Multiscale structure of calcium-and magnesium-silicate-hydrate gels. *J. Mater. Chem.* A 2, 12991–12998. doi:10.1039/c4ta02479f

Cizer, Ö., Rodriguez-Navarro, C., Ruiz-Agudo, E., Elsen, J., Van Gemert, D., and Van Balen, K. (2012). Phase and morphology evolution of calcium carbonate precipitated by carbonation of hydrated lime. *J. Mater. Sci.* 47, 6151–6165. doi:10.1007/s10853-012-6535-7

Delatte, D., Kaya, E., Kolibal, L. G., Mendon, S. K., Rawlins, J. W., and Thames, S. F. (2014). Synthesis and characterization of a soybean oil-based macromonomer. *J. Appl. Polym. Sci.* 131, app.40249. doi:10.1002/app.40249

Demchuk, Z., Shevchuk, O., Tarnavchyk, I., Kirianchuk, V., Lorenson, M., Kohut, A., et al. (2016). Free-radical copolymerization behavior of plant-oil-based vinyl monomers and their feasibility in latex synthesis. *ACS omega* 1, 1374–1382. doi:10.1021/acsomega.6b00308

 $EN\,1015\text{-}11\,(1999)$  . Methods of test for mortar for masonary - Part 11: Determination of flexural and compressive strength of hardened mortar.

EN 1015-18 (2003). Methods of test for mortar for masonry - part 18: determination of water absorption coefficient due to capillary action of hardened mortar.

EN 1015-3 (2000). Methods of test for mortar for masonry - part 3: determination of consistence of fresh mortar (by flow table).

EN 196-6 (2010). Methods of testing cement - part 6: determination of fineness

EN 197-1 (2013). Cement - part 1: composition, specifications and conformity criteria for common cements.

 $\rm EN$  2555 (2018). Plastics — resins in the liquid state or as emulsions or dispersions — determination of apparent viscosity using a single cylinder type rotational viscometer method.

EN 3251 (2003). Paints, varnishes and plastics - determination of non-volatile-matter content (ISO 3251:2003).

EN 6427 (2014). Plastics - determination of matter extractable by organic solvents (conventional methods) (ISO 6427:2013).

Eren, F., Gödek, E., Keskinateş, M., Tosun Felekoğlu, K., and Felekoğlu, B. (2017). Effects of latex modification on fresh state consistency, short term strength and long term transport properties of cement mortars. *Constr. Build. Mater.* 133, 226–233. doi:10.1016/j.conbuildmat.2016.12.080

Făcăoaru, I. (1970). "4 non-destructive testing of concrete in Romania," in Non-destructive testing of concrete and timber (Thomas Telford Publishing), 39–49.

- Fan, L., Xu, F., Wang, S., Yu, Y., Zhang, J., and Guo, J. (2023). A review on the modification mechanism of polymer on cement-based materials. *J. Mater. Res. Technol.* 26, 5816–5837. doi:10.1016/j.jmrt.2023.08.291
- Ferreira, G. R., Braquehais, J. R., da Silva, W. N., and Machado, F. (2015). Synthesis of soybean oil-based polymer lattices via emulsion polymerization process. *Ind. Crops Prod.* 65, 14–20. doi:10.1016/j.indcrop.2014.11.042
- Flory, P. J., and Rehner, J. (1943). Statistical mechanics of cross-linked polymer networks I. Rubberlike elasticity. *J. Chem. Phys.* 11, 512–520. doi:10.1063/1.1723791
- Fox, T. G., and Flory, P. J. (1950). Second-order transition temperatures and related properties of polystyrene. I. Influence of molecular weight. *J. Appl. Phys.* 21, 581–591. doi:10.1063/1.1699711
- Guerrero-Santos, R., Saldívar-Guerra, E., and Bonilla-Cruz, J. (2013). "Free radical polymerization," in *Handbook of polymer synthesis, characterization, and processing*. Editors E. Saldívar-Guerra, and E. Vivaldo-Lima (Hoboken, NJ, USA: John Wiley and Sons, Inc.), 65–83. doi:10.1002/9781118480793.ch4
- Haq, I. U., Elahi, A., Nawaz, A., Shah, S. A. Q., and Ali, K. (2022). Mechanical and durability performance of concrete mixtures incorporating bentonite, silica fume, and polypropylene fibers. *Constr. Build. Mater.* 345, 128223. doi:10.1016/j.conbuildmat.2022.128223
- Hellgren, A.-C., Weissenborn, P., and Holmberg, K. (1999). Surfactants in waterborne paints. *Prog. Org. coatings* 35, 79–87. doi:10.1016/s0300-9440(99)00013-2
- Ho, Y. H., Parthiban, A., Thian, M. C., Ban, Z. H., and Siwayanan, P. (2022). Acrylated biopolymers derived *via* epoxidation and subsequent acrylation of vegetable oils. *Int. J. Polym. Sci.* 2022, 1–12. doi:10.1155/2022/6210128
- Ismail, M., Muhammad, B., Yatim, J. M., Noruzman, A. H., and Soon, Y. W. O. O. (2011). Behavior of concrete with polymer additive at fresh and hardened states. *Procedia Eng.* 14, 2230–2237. doi:10.1016/j.proeng.2011.07.281
- ISO 2115 (1996). Plastics polymer dispersions determination of white point temperature and minimum film-forming temperature.
- Jenni, A., Zurbriggen, R., Holzer, L., and Herwegh, M. (2006). Changes in microstructures and physical properties of polymer-modified mortars during wet storage. *Cem. Concr. Res.* 36, 79–90. doi:10.1016/j.cemconres.2005.06.001
- Jiang, C., Huang, S., Gao, P., and Chen, D. (2018). Experimental study on the bond and durability properties of mortar incorporating polyacrylic ester and silica fume. *Adv. Cem. Res.* 30, 56–65. doi:10.1680/jadcr.17.00053
- Knapen, E., and Van Gemert, D. (2015). Polymer film formation in cement mortars modified with water-soluble polymers. *Cem. Concr. Compos.* 58, 23–28. doi:10.1016/j.cemconcomp.2014.11.015
- Kolář, M., Honzíček, J., Podzimek, Š., Knotek, P., Hájek, M., Zárybnická, L., et al. (2023a). Derivatives of linseed oil and camelina oil as monomers for emulsion polymerization. *J. Mater. Sci.* 58, 15558–15575. doi:10.1007/s10853-023-08969-4
- Kolář, M., Machotová, J., Hájek, M., Honzíček, J., Hájek, T., and Podzimek, Š. (2023b). Application of vegetable oil-based monomers in the synthesis of acrylic latexes *via* emulsion polymerization. *Coatings* 13, 262. doi:10.3390/coatings13020262
- Kong, X.-M., Wu, C.-C., Zhang, Y.-R., and Li, J.-L. (2013). Polymer-modified mortar with a gradient polymer distribution: preparation, permeability, and mechanical behaviour. *Constr. Build. Mater.* 38, 195–203. doi:10.1016/j.conbuildmat.2012.07.080
- Lathi, P., and Mattiasson, B. (2007). Green approach for the preparation of biodegradable lubricant base stock from epoxidized vegetable oil. *Appl. Catal. B Environ.* 69, 207–212. doi:10.1016/j.apcatb.2006.06.016
- Laurentino, L. S., Medeiros, A. M. M. S., Machado, F., Costa, C., Araújo, P. H. H., and Sayer, C. (2018). Synthesis of a biobased monomer derived from Castor oil and copolymerization in aqueous medium. *Chem. Eng. Res. Des.* 137, 213–220. doi:10.1016/j.cherd.2018.07.014
- Łaźniewska-Piekarczyk, B. (2013). Examining the possibility to estimate the influence of admixtures on pore structure of self-compacting concrete using the air void analyzer. *Constr. Build. Mater.* 41, 374–387. doi:10.1016/j.conbuildmat.2012.11.100
- Li, G., Morlor, C. S., Leung, C., and Wang, H. (2021a). Mechanical properties and fractal analysis of cement mortar incorporating styrene-butadiene rubber latex and carboxylated MWCNTs. *Constr. Build. Mater.* 309, 125175. doi:10.1016/j.conbuildmat.2021.125175
- Li, P., Lu, W., An, X., Zhou, L., and Du, S. (2021b). Effect of epoxy latexes on the mechanical behavior and porosity property of cement mortar with different degrees of hydration and polymerization. *Mater. (Basel)* 14, 517. doi:10.3390/ma14030517
- Liang, C., Li, B., Guo, M.-Z., Hou, S., Wang, S., Gao, Y., et al. (2024). Effects of early-age carbonation curing on the properties of cement-based materials: a review. *J. Build. Eng.* 84, 108495. doi:10.1016/j.jobe.2024.108495
- Liu, B., Shi, J., Sun, M., He, Z., Xu, H., and Tan, J. (2020). Mechanical and permeability properties of polymer-modified concrete using hydrophobic agent. *J. Build. Eng.* 31, 101337. doi:10.1016/j.jobe.2020.101337
- Liu, Q., Lu, Z., Xu, J., Li, Z., and Sun, G. (2023a). Insight into the *in situ* copolymerization of monomers on cement hydration and the mechanical performance of cement paste. *J. Sustain. Cem. Mater.* 12, 736–750. doi:10.1080/21650373.2022.2118190

Liu, Z., Li, S., Sui, S., Liu, A., Geng, Y., Chen, X., et al. (2023b). Preparation of hydroxylated hexagonal boron nitride/isobutyltriethoxysilane hybrid latices for improved waterproofing performance of cement coating. *Constr. Build. Mater.* 404, 133232. doi:10.1016/j.conbuildmat.2023.133232

- Lothenbach, B., and Winnefeld, F. (2006). Thermodynamic modelling of the hydration of Portland cement. *Cem. Concr. Res.* 36, 209–226. doi:10.1016/j.cemconres.2005.03.001
- Luo, D., Li, F., and Niu, D. (2024). Study on the deterioration of concrete performance in saline soil area under the combined effect of high low temperatures, chloride and sulfate salts. *Cem. Concr. Compos.* 150, 105531. doi:10.1016/j.cemconcomp.2024.105531
- Machotova, J., Podzimek, S., Kvasnicka, P., Zgoni, H., Snuparek, J., and Cerny, M. (2016). Effect of molar mass on film-forming properties of self-crosslinking latexes based on structured acrylic microgels. *Prog. Org. Coatings* 92, 23–28. doi:10.1016/j.porgcoat.2015.12.003
- Machotová, J., Kalendová, A., Steinerová, D., Mácová, P., Šlang, S., Šňupárek, J., et al. (2021). Water-resistant latex coatings: tuning of properties by polymerizable surfactant, covalent crosslinking and nanostructured zno additive. *Coatings* 11, 347. doi:10.3390/coatings11030347
- Machotová, J., Pokorný, J., Zárybnická, L., and Ševčík, R. (2025). Effect of polymerizable ionic surfactant in the acrylic latex additive on advanced properties of Portland cement-based mortars. *Constr. Build. Mater.* 487, 142079. doi:10.1016/j.conbuildmat.2025.142079
- Malhotra, V. M., and Carino, N. J. (2003). Handbook on nondestructive testing of concrete. Boca Raton: CRC Press.
- Mecking, S. (2004). Nature or petrochemistry? biologically degradable materials. Angew. Chem. Int. Ed. 43, 1078–1085. doi:10.1002/anie.200301655
- Moreno, M., Lampard, C., Williams, N., Lago, E., Emmett, S., Goikoetxea, M., et al. (2015). Eco-paints from bio-based fatty acid derivative latexes. *Prog. Org. Coatings* 81, 101–106. doi:10.1016/j.porgcoat.2015.01.001
- Neves, J. S., Valadares, L. F., and Machado, F. (2018). Tailoring acrylated soybean oil-containing terpolymers through emulsion polymerization. *Colloids Interfaces* 2, 46. doi:10.3390/colloids2040046
- Ohama, Y. (1998). Polymer-based admixtures. Cem. Concr. Compos. 20, 189–212. doi:10.1016/s0958-9465(97)00065-6
- Pang, Y., Wang, H., Yang, L., Tang, Q., Wang, Q., and Wang, G. (2025). Sulfate freeze-thaw resistance enhancement of cement mortar *via* a developed hydrophobic mica powder. *I. Sustain. Cem. Mater.* 14, 578–592. doi:10.1080/21650373.2024.2442083
- Pokorný, J., Ševčík, R., Šál, J., and Zárybnická, L. (2021a). Lightweight blended building waste in the production of innovative cement-based composites for sustainable construction. *Constr. Build. Mater.* 299, 123933. doi:10.1016/j.conbuildmat.2021.123933
- Pokorný, J., Ševčík, R., Šál, J., Zárybnická, L., and Žák, J. (2021b). Lightweight concretes with improved water and water vapor transport for remediation of damp induced buildings. *Mater. (Basel)* 14, 5902. doi:10.3390/ma14195902
- Quirino, R. L., Kessler, M. R., Netravali, A. N., and Pastore, C. M. (2015). "Vegetable oil-based resins and composites," in *Sustainable composites fibers, resins and applications* (Boca Raton: DEStech Publications).
- Ragauskas, A. J., Williams, C. K., Davison, B. H., Britovsek, G., Cairney, J., Eckert, C. A., et al. (2006). The path forward for biofuels and biomaterials. *Sci.* (80) 311, 484–489. doi:10.1126/science.1114736
- Ramli, M., and Akhavan Tabassi, A. (2012). Effects of polymer modification on the permeability of cement mortars under different curing conditions: a correlational study that includes pore distributions, water absorption and compressive strength. *Constr. Build. Mater.* 28, 561–570. doi:10.1016/j.conbuildmat.2011.09.004
- Rodriguez-Navarro, C., Ilić, T., Ruiz-Agudo, E., and Elert, K. (2023). Carbonation mechanisms and kinetics of lime-based binders: an overview. *Cem. Concr. Res.* 173, 107301. doi:10.1016/j.cemconres.2023.107301
- Saldívar-Guerra, E., and Vivaldo-Lima, E. (2013). Introduction to polymers and polymer types. *Handb. Polym. Synth. Charact. Process.*, 1–14. doi:10.1002/9781118480793.ch1
- Scrivener, K., Ouzia, A., Juilland, P., and Mohamed, A. K. (2019). Advances in understanding cement hydration mechanisms. *Cem. Concr. Res.* 124, 105823. doi:10.1016/j.cemconres.2019.105823
- Ševčík, R., Machotová, J., Zárybnická, L., Mácová, P., and Viani, A. (2023). Aqueous polyacrylate latex nanodispersions used as consolidation agents to improve mechanical properties of prague sandstone. *J. Cult. Herit.* 62, 412–421. doi:10.1016/j.culher.2023.06.021
- Sevelsted, T. F., and Skibsted, J. (2015). Carbonation of C–S–H and C–A–S–H samples studied by 13C, 27Al and 29Si MAS NMR spectroscopy. *Cem. Concr. Res.* 71, 56–65. doi:10.1016/j.cemconres.2015.01.019
- Shah, H. A., Yuan, Q., and Zuo, S. (2021). Air entrainment in fresh concrete and its effects on hardened concrete-a review. *Constr. Build. Mater.* 274, 121835. doi:10.1016/j.conbuildmat.2020.121835

Shi, C., Wang, P., Ma, C., Zou, X., and Yang, L. (2021). Effects of SAE and SBR on properties of rapid hardening repair mortar. *J. Build. Eng.* 35, 102000. doi:10.1016/j.jobe.2020.102000

Silva, D. A. D., Roman, H. R., and Gleize, P. J. P. (2002). Evidences of chemical interaction between EVA and hydrating Portland cement. *Cem. Concr. Res.* 32, 1383–1390. doi:10.1016/s0008-8846(02)00805-0

Sumra, Y., Payam, S., and Zainah, I. (2020). The pH of cement-based materials: a review. J. Wuhan. Univ. Technol. Sci. 35, 908–924. doi:10.1007/s11595-020-2337-y

Sun, K., Wang, S., Zeng, L., and Peng, X. (2019). Effect of styrene-butadiene rubber latex on the rheological behavior and pore structure of cement paste. *Compos. Part B Eng.* 163, 282–289. doi:10.1016/j.compositesb.2018.11.017

Teramoto, N. (2011). "Chapter 2. Synthetic green polymers from renewable monomers," in *Green chemistry series*. Editors S. K. Sharma, and A. Mudhoo (Cambridge: Royal Society of Chemistry), 22–78. doi:10.1039/9781849733458-00022

Tobing, S. D., and Klein, A. (2001). Molecular parameters and their relation to the adhesive performance of emulsion acrylic pressure-sensitive adhesives. II. Effect of crosslinking. *J. Appl. Polym. Sci.* 79, 2558–2564. doi:10.1002/1097-4628(20010401)79:14<2558::AID-APP1065>3.0.CO;2-Y

Tosun, K., and Baradan, B. (2010). Effect of ettringite morphology on DEF-Related expansion. *Cem. Concr. Compos.* 32, 271–280. doi:10.1016/j.cemconcomp.2010.01.002

Tukimat, N. N. A., Sarbini, N. N., Ibrahim, I. S., Ma, C. K., and Mutusamy, K. (2017). Fresh and hardened state of polymer modified concrete and mortars - a review. *MATEC Web Conf.* 103, 01025. doi:10.1051/matecconf/201710301025

Ukrainczyk, N., and Rogina, A. (2013). Styrene-butadiene latex modified calcium aluminate cement mortar. *Cem. Concr. Compos.* 41, 16–23. doi:10.1016/j.cemconcomp.2013.04.012

Van Tittelboom, K., and De Belie, N. (2013). Self-healing in cementitious materials—A review. *Mater. (Basel)* 6, 2182–2217. doi:10.3390/ma6062182

Vandenburg, H. J., Clifford, A. A., Bartle, K. D., Carlson, R. E., Carroll, J., and Newton, I. D. (1999). A simple solvent selection method for accelerated solvent extraction of additives from polymers. *Analyst* 124, 1707–1710. doi:10.1039/a904631c

Wagner, H. B. (1965). Polymer-modified hydraulic cements. *Ind. Eng. Chem. Prod. Res. Dev.* 4, 191–196. doi:10.1021/i360015a011

Wang, R., and Wang, P. (2010). Function of styrene-acrylic ester copolymer latex in cement mortar. *Mater. Struct.* 43, 443–451. doi:10.1617/s11527-009-9501-3

Wang, R., and Wang, P.-M. (2011). Action of redispersible vinyl acetate and versatate copolymer powder in cement mortar. *Constr. Build. Mater.* 25, 4210–4214. doi:10.1016/j.conbuildmat.2011.04.060

Wiley-VCH (2002). Polymer dispersions and their industrial applications. Weinheim: Wiley VCH.

Williams, C., and Hillmyer, M. (2008). Polymers from renewable resources: a perspective for a special issue of polymer reviews. *Polym. Rev.* 48, 1–10. doi:10.1080/15583720701834133

Wu, Y., and Li, K. (2018). Acrylated epoxidized soybean oil as a styrene replacement in a dicyclopentadiene-modified unsaturated polyester resin. *J. Appl. Polym. Sci.* 135, 46212. doi:10.1002/app.46212

Wu, L., Wu, Z., Weng, L., Liu, Y., and Liu, Q. (2023). Investigation on basic properties and microscopic mechanisms of polyacrylate latex modified cement grouting material for water blocking and reinforcement. *Constr. Build. Mater.* 409, 133872. doi:10.1016/j.conbuildmat.2023.133872

Wu, L., Wu, Z., Weng, L., Liu, Y., Chu, Z., and Chen, J. (2024). Comparative analysis of polyacrylate latex modified cement grout for water blocking and rock reinforcement with six alternative materials. Constr. Build. Mater. 429, 136377. doi:10.1016/j.conbuildmat.2024.136377

Wuzella, G., Mahendran, A. R., Müller, U., Kandelbauer, A., and Teischinger, A. (2012). Photocrosslinking of an acrylated epoxidized linseed oil: Kinetics and its application for optimized wood coatings. *J. Polym. Environ.* 20, 1063–1074. doi:10.1007/s10924-012-0511-9

Yao, K., and Tang, C. (2013). Controlled polymerization of next-generation renewable monomers and beyond. *Macromolecules* 46, 1689–1712. doi:10.1021/ma3019574

Zarybnicka, L., Machotová, J., Mácová, P., Machová, D., and Viani, A. (2021). Design of polymeric binders to improve the properties of magnesium phosphate cement. *Constr. Build. Mater.* 290, 123202. doi:10.1016/j.conbuildmat. 2021.123202

Zárybnická, L., Pokorný, J., Machotová, J., Ševčík, R., Šál, J., and Viani, A. (2023). Study of keto-hydrazide crosslinking effect in acrylic latex applied to Portland cements with respect to physical properties. *Constr. Build. Mater.* 375, 130897. doi:10.1016/j.conbuildmat.2023.130897

Zhang, P., Liu, G., Pang, C., Yan, X., and Qin, H. (2017). Influence of pore structures on the frost resistance of concrete. *Mag. Concr. Res.* 69, 271–279. doi:10.1680/jmacr.15.00471

Zhang, X., Li, G., and Song, Z. (2019). Influence of styrene-acrylic copolymer latex on the mechanical properties and microstructure of Portland Cement/calcium aluminate Cement/gypsum cementitious mortar. Constr. Build. Mater. 227, 116666. doi:10.1016/j.conbuildmat.2019. 08.047